Tunable microwave dielectric properties in SrO-V2O5 system through compositional modulation

Journal:	*Journal of the American Ceramic Society*
Manuscript ID	JACERS-44698.R2
Manuscript Type:	Rapid Communication
Date Submitted by the Author:	n/a
Complete List of Authors:	Li, Chunchun; Guilin University of Technology, College of Information Science and Engineering; Guilin University of Technology, Key laboratory of New Processing Technology for Nonferrous Metal and MaterialsMinistry of Education Yin, Changzhi; State Key Laboratory Breeding Base of Nonferrous metals and specific Materials Processing, Guangxi universities key laboratory of non-ferrous metal oxide electronic functional materials and devices, College of Material Science and Engineering, Guilin University of Technology Deng, Ming; Guilin University of Technology, College of Information Science and Engineering Shu, Longlong; Nanchang University, School of Materials Science and Engineering Khaliq, Jibran; University of Northumbria at Newcastle
Keywords:	ceramic matrix composites, dielectric materials/properties, LTCC, microwaves
Author-supplied Keyword: If there is one additional keyword you would like to include that was not on the list, please add it below::	

Tunable microwave dielectric properties in SrO-V_2O_5 system through compositional modulation

Chunchun Li[1, 2*], Changzhi Yin[2], Ming Deng[1], Longlong Shu[3], Jibran Khaliq[4**]

[1] *College of Information Science and Engineering, Guilin University of Technology, Guilin, 541004, China*

[2]*State Key Laboratory Breeding Base of Nonferrous metals and specific Materials Processing, Guangxi universities key laboratory of non-ferrous metal oxide electronic functional materials and devices, College of Material Science and Engineering, Guilin University of Technology, Guilin, 541004, China*

[3]*School of Materials Science and Engineering, Nanchang University, Nanchang 330031, People's Republic of China*

[4]*Department of Mechanical and Construction Engineering, Faculty of Engineering and Environment, Northumbria University at Newcastle, NE1 8ST, UK*

Abstract

Adjustment on resonance frequency stability against the sintering temperature of $Sr_3V_2O_8$ was realized through adjusting the Sr:V mole ratio. Effects of Sr:V ratio on sintering behavior and dielectric properties of $Sr_3V_2O_8$ were studied. The sintering temperature was sucessfully reduced to 950 °C from 1150 °C. With increasing vanadium content, both relative permittivity and quality factor decreased, while the temperature coefficient of resonance frequency shifted from positive to negative values. Especially, a near-zero τ_f of -1.1 ppm/°C along with a low permittivity (ε_r) of 9.8 and a quality factor $Q \times f$ of 24,120 GHz was successfully achieved in $Sr_{3-y}V_2O_{8-y}$ ceramic (y = 0.6, sintered at 950 °C). The wide compositional and processing adjustment window, favorable dielectric performances, and good chemical compatibility with silver render $Sr_{3-y}V_2O_{8-y}$ ceramics potential candidates in multilayer electronic devices.

Keywords: Ceramics; Dielectric properties; Microwave resonance; Composite

* Corresponding Author, lichunchun2003@126.com, **Jibran.khaliq@northumbria.ac.uk

ceramics

1. Introduction

The developments of commercial wireless technologies, especially the fifth-generation (5G) telecommunication, Internet of Things (IoTs) and military radar systems, have expanded the operating frequency to the millimeter-wave range. This new technological paradigm brings out the increasing demands of high-speed signal propagation at high-frequency regions [1-4]. For ceramics used as substrates, low permittivity (ε_r < 15) is required for fast signal transmission and minimizing the crosscoupling between the substrates and the conductors [5-7]. Other properties such as high quality factors ($Q \times f$) and near-zero temperature coefficient of resonant frequency (τ_f) are also essential for practical applications [8-10]. To date, a large number of dielectric materials have been reported, however, only a few numbers of available options could meet the combination requirements simultaneously. Thus, developing new materials with desired microwave dielectric properties is still a challenge.

To reduce the permittivity, two possible approaches have been proposed in the literatures [11, 12], one of which is to decrease the number of dipoles while the second is to lower the dipole strength. The former method involves lowering the density through introduction of porosity. This however sacrifices mechanical strength and thermal conductivity while increasing dielectric loss. Lowering the dipole strength is more desirable through introducing covalent bond. To date, a number of promising low-permittivity materials (ε_r < 15) have been reported. All of those materials have

tetrahedral unit cell, such as borates, silicates, phosphates, and vanadates [3, 12-14]. Amongest them, vanadates have attracted considerable attention due to cheap raw materials, simple synthetic process, and good microwave dielectric properites [15-18]. For example, alkaline earth orthovanadates, $M_3(VO_4)_2$ (M = Mg, Ba, Sr) are promising candidates with low dielectric loss and low-ε_r for high-frequency application [17-19]. $Mg_3(VO_4)_2$ sintered at 950 °C possesses ε_r = 9.3, $Q\times f$ = 65,540 GHz and τ_f = -89.5 ppm/°C [19], and $Ba_3(VO_4)_2$ exhibited good dielectric performances with $\varepsilon_r \sim 11.3$, $Q\times f$ ~ 62,347 GHz and $\tau_f \sim$ 28.8 ppm/°C when sintered at 1400 °C [20]. In our previous work, $Ba_{3-x}Sr_x(VO_4)_2$ solid solution series were reported to have promising microwave dielectric properties with ε_r = 11-16, $Q\times f$ = 40,000-66,000GHz, and τ_f = 20-70 ppm/°C [21]. Particularly, $Sr_3(VO_4)_2$ has the lowest densification temperature (~ 1150 °C) along with a combination of promising dielectric performances with a high quality factor of 44,340 GHz and a low dielectric permittivity of 12.2. The high sintering temperature (>1000 ^oC) and relatively large positive τ_f value (~ +63.5 ppm/^oC), however, still limits its potential utilization in low temperature cofired ceramics (LTCC) application in which the ceramic layers should be cofired with the inner electrodes (generally silver) [22]. Thus, reduction in sintering temperature to below the melting temperature of silver (961 ^oC) and tailoring τ_f to near-zero is necessary for $M_3(VO_4)_2$ [23-25].

According to the binary phase diagram of SrO-V_2O_5, there are two stable phases $Sr_2V_2O_7$ with triclinic structure and $Sr_3(VO_4)_2$ and both of the phases can coexist [26]. Importantly, one of the advantages of $Sr_2V_2O_7$ is to have a negative τ_f value ~ -34.8 ppm/°C which can behave as a τ_f compensator for $Sr_3(VO_4)_2$. Both phases can coexist

by adjusting Sr:V mole ratio in the binary SrO-V_2O_5 system to complement each other [27]. Based on this rationale, this paper proposed the formation of the second phase to compensate τ_f value in-situ by compositional modification, a reliable and simple method, which was validated and verified in $Sr_{3-y}V_2O_{8-y}$ ($0 \leq y \leq 1$) ceramics system. A series of different Sr:V ratio compounds in the $Sr_{3-y}V_2O_{8-y}$ (y = 0.2-0.8) system were prepared and characterized for the relationships between the phase composition and microwave dielectric properties.

2. Experimental Procedure

2.1 *Sample preparation*

$Sr_{3-y}V_2O_{8-y}$ (y = 0.2, 0.4, 0.6, 0.8) ceramics were prepared via conventional solid-state method from individual reagent-grade oxide powders: $SrCO_3$, (> 99.95%, Guo-Yao Co., Ltd Shanghai, China) and NH_4VO_3 (> 99.9%, Guo-Yao Co., Ltd Shanghai, China). The powders were weighted according to the stoichiometric composition of $Sr_{3-y}V_2O_{8-y}$, and ball milled in alcohol medium for 6 h in nylon battle with zirconia balls. After drying the slurry at 120 °C for 1 h, the obtained powders were calcined at 850 °C for 6 h in air. The calcined powders were ball-milled again for 6 h followed by cold-pressing into cylinders (10 mm in diameter and 6 mm in thickness) in a steel die under a pressure of 200 MPa with polyvinyl alcohol (PVA, 10 vol.%) as s binder. The $Sr_{3-y}V_2O_{8-y}$ pellets were sintering at in the range of 900-1150 °C for 6h in the air.

2.2 *Characteristics*

The crystal structure and phase(s) of the specimens were analyzed using X-ray diffraction (Cu*Kα1*, 1.54059 Å, Model X'Pert PRO, PANalytical, Almelo, Holland).

The diffraction patterns were taken at room temperature in the range of 10 °-80 ° by step scans. The bulk density was determined by the Archimedes' method and the theoretical density was obtained by the following equation:

$$\rho_{th} = \frac{\omega_1 + \omega_2}{\omega_1/\rho_1 + \omega_2/\rho_2} \quad (1)$$

where ω_1, ω_2, and ρ_1, ρ_2 are the mass fractions and theoretical density of $Sr_2V_2O_7$ and $Sr_3(VO_4)_2$, respectively.

The surface morphologies of the sintered samples were observed by scanning electron microscope (FE-SEM, Model S4800, Hitachi, Japan). The relative permittivity (ε_r) and quality factor ($Q \times f$) of the samples were measured using a network analyzer (Model N5230A, Agilent Co., Palo Alto, America). The temperature coefficient of resonant frequency (τ_f) was measured by noting the temperature shift of the resonance scope in the temperature range of 25-85 °C using a temperature chamber (Delta 9039, Delta Design, San Diego, CA) and were calculated as follows:

$$\tau_f\,(\text{ppm/}^{o}\text{C}) = \frac{f_2 - f_1}{f_1(T_2 - T_1)} \times 10^6 \quad (2)$$

where, f_1 and f_2 represent resonant frequencies at temperatures T_1 and T_2, respectively.

3. Results and discussion

In order to get a clear understanding of the chemical reaction happening within $Sr_{3-y}V_2O_{8-y}$ system, thermal analysis was carried out. Fig. 1(a) shows the TG/DSC thermograph of the mixed precursor of the y = 0.2 sample. Three endothermic peaks between 150 °C to 450 °C were observed in the DSC curve, accompanied by a total mass loss of nearly 8% on the TGA curve. These three peaks, located at 200 °C, 225 °C and 370 °C correspond to the gradual decomposition of NH_4VO_3 into V_2O_5 and NH_3

with the first as the primary decomposition process. A broad exothermic peak around 527 °C can be related to the chemical reaction of V_2O_5 with $SrCO_3$ to form $Sr_2V_2O_7$ and/or $Sr_3V_2O_8$ with mass loss of nearly 8% due to the release of carbon dioxide. The endothermic peak at 880 °C is associated with the complete decomposition of $SrCO_3$. Fig. 1(b) shows the XRD pattern of the y = 0.2 sample sintered at 860 and 960 °C. A peak belonging to $SrCO_3$ is visible at 860 °C, which disappeared at 960 °C, hence confirming the thermal analysis.

Fig. 2(a) illustrates the XRD patterns of $Sr_{3-y}V_2O_{8-y}$ (y = 0.2-0.8) ceramics sintered at 950 °C. Within the range of $0.2 \leq y \leq 0.8$, only two main crystalline phases, $Sr_2V_2O_7$ with a space group P-1 (No. 2) and $Sr_3(VO_4)_2$ were observed and the volume fraction of $Sr_2V_2O_7$ increased with increasing y value, as listed in Table 1, which was verified based on the bi-phase Rietveld refinement. As representatives, Figs. 2(b, c) show the refined XRD patterns with y = 0.2 and y = 0.8. The reasonable reliability factors indicate that a mixed-phase of $Sr_3(VO_4)_2$ and $Sr_2V_2O_7$ were obtained in all samples. Additionally, Fig. 2(d) shows the change of relative density as a function of y value and phase fraction of $Sr_2V_2O_7$ calculated from refinement. All the sintered $Sr_{3-y}V_2O_{8-y}$ samples exhibited a relative density of over 95% and an upward trend with an increase in y value, indicating that the increment of V_2O_5 content facilitates densification of $Sr_{3-y}V_2O_{8-y}$. The phase content of $Sr_2V_2O_7$ increased from 20.47% to 81.31%, which is very close to the theoretical values (17.88% to 77.7%) obtained from the nominal formula $Sr_{3-y}V_2O_{8-y}$.

Fig. 3(a-d) present the SEM images of $Sr_{3-y}V_2O_{8-y}$ (y = 0.2-0.8) sintered at their

optimum temperatures. Following the high relative density (over 95%, Table 1), all the samples show well-densified microstructures. It can be seen that two different shapes of grains (round and columnar grains) coexisted in the samples in the composition range studied. Fig. 3(e, f) presented the elemental content in different grains (spot 1 and 2) captured using EDS. The Sr/V ratio of the columnar phases is approximately 1.52, which is close to the composition of $Sr_3V_2O_8$, while Sr/V ratio for the round phase is around 1.01, corresponding to $Sr_2V_2O_7$ phase. The EDS results confirmed that the round-like grains were $Sr_2V_2O_7$ phase and the columnar-like grains were $Sr_3V_2O_8$ phase.

The microwave dielectric properties (ε_r, $Q\times f$, and τ_f) of $Sr_{3-y}V_2O_{8-y}$ (y = 0.2-0.8) ceramics exhibited a downward trend with increasing y value as shown in Fig. 4. Particularly, the τ_f value of the $Sr_{3-y}V_2O_{8-y}$ ceramics decreased from +48.7 ppm/°C to -20.1 ppm/°C. $Sr_{3-y}V_2O_{8-y}$ composite having y = 0.6 and sintered at 950 °C demonstrated a near-zero τ_f of -1.1 ppm/°C, along with ε_r of 9.8 and quality factor $Q\times f$ of 24,120 GHz. According to the empirical Lichtenecker mixing rule for a two-phase composite, the effective ε_r, $Q\times f$, and τ_f values can be theoretically estimated by the following equations [28]:

$$\varepsilon^n = V_1\varepsilon_1^n + V_2\varepsilon_2^n \quad (-1\leq n\leq 1) \qquad (3)$$

$$\tau_f = v_1\tau_{f1} + v_2\tau_{f2} \qquad (4)$$

$$\frac{1}{Q} = \frac{v_1}{Q_1} + \frac{v_2}{Q_2} \qquad (5)$$

where ε_1 and ε_2 are the respective permittivities of $Sr_3(VO_4)_2$ and $Sr_2V_2O_7$ phase; τ_{f1} and τ_{f2} are the τ_f values of the pure $Sr_3(VO_4)_2$ and $Sr_2V_2O_7$ phase, V_1 and V_2 ($V_1 + V_2 = 1$) are the volume fractions of the corresponding phases. And n = 1 or -1 correspond to

the parallel and series mixing law, respectively. When n approaches 0, Eq. (3) becomes logarithmic, usually used for randomly distributed composites:

$$ln\,\varepsilon = V_1 ln\,\varepsilon_1 + V_2 ln\,\varepsilon_2 \quad (6)$$

As shown in Fig. 4(a), the measured values of ε_r for $Sr_{3-y}V_2O_{8-y}$ (y = 0.0-1.0) composites are matched with values calculated using equations of parallel or series mixing law, and Eq. (6). This indicates that the measured values of ε_r follow the logarithmic mixing law with the respective volume fraction. The theoretical $Q\times f$ and τ_f values of $Sr_{3-y}V_2O_{8-y}$ (y = 0.2-0.8) are calculated using the Eq. (4) and (5) and shown in Figs. 4(b, c). The measured $Q\times f$ and τ_f values were in agreement with the theoretical values, confirming that the dielectric properties can be conveniently and precisely tailored by this method.

The low sintering temperature (950 ˚C) of sample with y = 0.6 enables its potential application in LTCC technology. To evaluate the chemical compatibility with silver, cofiring was carried out between the y = 0.6 and 20 wt.% Ag powders at 950 ˚C for 2 h. As shown, XRD pattern recorded on the cofired sample only exhibits peaks of silver (ICDD No. 87-0717), $Sr_3V_2O_8$, and $Sr_2V_2O_7$. In addition, backscattered electron image (BEI) shows distinguish grains with different element contrasts and the bright grains were verified as silver by EDS analysis. These results suggest that the present ceramics have a good chemical compatibility with Ag electrode, rendering their potential use in LTCC technology.

4. Conclusions

To tailor the temperature coefficient of resonance frequency and lower the sintering temperature of $Sr_3V_2O_8$, in-situ composite formation through modified Sr:V

ratio was proposed and a series of $Sr_{3-y}V_2O_{8-y}$ were prepared. Successful reduction in sintering temperature was achieved from 1150 °C to 950 °C, rendering their future possible application in LTCC technology. Microwave dielectric properties can also be tuned by varying the Sr:V ratio. In particular, a composition with $y = 0.6$ sintered at 950 °C possessed a near-zero τ_f of -1.1 ppm/°C, along with ε_r of 9.8 and quality factor $Q \times f$ of 24,120 GHz. This work paves the way for $Sr_3(VO_4)_2$ ceramics to utilize in multilayer electronic devices.

Acknowledgments

This work was supported by the Natural Science Foundation of Guangxi Zhuang Autonomous Region (No 2018GXNSFAA281253).

References

[1] Sebastian MT, Jantunen H, Low loss dielectric materials for LTCC applications: a review. Int. Mater. Rev. 2008; 53: 57-90.

[2] Song XQ, Du K, Li J, Muhammad R, Lu WZ, Wang XC, et al. Lattice structures and microwave dielectric properties of novel low-permittivity $Ba_{1-x}Sr_xZnSi_3O_8$ ceramics. J. Am. Ceram. Soc. 2019; 112: 178-181.

[3] Zhou D, Pang LX, Wang DW, Qi ZM, Reaney IM, High quality factor, ultralow sintering temperature $Li_6B_4O_9$ microwave dielectric ceramics with ultralow density for antenna substrates. ACS Sustainable Chem. Eng. 2018; 6: 11138-11143.

[4] Zhang SB, Shi LW, Zhang LY, Zhu HY, Xia WS, Synthesis and microwave dielectric properties of new high quality Mg_2NdNbO_6 ceramics. J. Am. Ceram. Soc. 2018; 101: 1014-1019.

[5] George S, Sebastian MT, Synthesis and microwave dielectric properties of novel Temperature Stable High Q $Li_2ATi_3O_8$ (A=Mg, Zn) Ceramics. J. Am. Ceram. Soc. 2010; 30: 2585-2592.

[6] Li CC, Xiang HC, Xu MY, Tang Y, Fang L, Li_2AGeO_4 (A = Zn, Mg): Two novel low-permittivity microwave dielectric ceramics with olivine structure. J. Eur. Ceram. Soc. 2018; 38: 1524-1528.

[7] Shi F, Yang J, Liu Q, Qi ZM, Sun H, Crystal structure, lattice vibrational characteristic, and dielectric property of $Nd(Mg_{1/2}Sn_{1/2})O_3$ ceramic. Mater. Chem. Phys. 2017; 200: 9-15.

[8] Li CC, YinCZ, Chen JQ, Xiang HC, Tang Y, Fang L, Crystal structure and dielectric properties of germanate melilites $Ba_2MGe_2O_7$ (M= Mg and Zn) with low permittivity. J. Eur. Ceram. Soc. 2018; 38: 5246-5251.

[9] Liu B, Hu CC, Huang YH, Bafrooei HB, Song KX, Crystal structure, infrared reflectivity spectra and microwave dielectric properties of $CaAl_2O_4$ ceramics with low permittivity. J. Alloys Compd. 2019; 791: 1033-1037.

[10] Ullah A, Liu H, Hao H, Iqbal J, Yao Z, Cao M, Influence of TiO_2 additive on sintering temperature and microwave dielectric properties of $Mg_{0.90}Ni_{0.1}SiO_3$ ceramics. J. Eur. Ceram. Soc. 2017;37: 3045-3049.

[11] Shamiryan D, Abell T, Iacopi F, Maex K, Low-K dielectric materials. 7th Philadelphia, PA: Materialstoday; 2004.

[12] Bian JJ, Sun XQ, Xie YR, Structural evolution, sintering behavior and microwave dielectric properties of $Al_{(1-x)}(Si0.5Zn0.5)_xPO_4$ ceramics. J. Eur. Ceram. Soc. 2019; 39: 4139-4143.

[13] Chen D, Luo F, Gao L, Zhou WC, Zhu DM, Dielectric and microwave absorption properties of divalent-doped $Na_3Zr_2Si_2PO_{12}$ ceramics. J. Eur. Ceram. Soc. 2018; 38: 4440-4445.

[14] Xiang HC, Li CC, Tang Y, Fang L, Two novel ultralow temperature firing microwave dielectric ceramics $LiMVO_6$ (M = Mo, W) and their chemical compatibility with metal electrodes. J. Eur. Ceram. Soc. 2017; 37: 3959-3963.

[15] Wang Y, Zuo RZ, Zhang C, Zhang J, Zhang TW, Low-temperature-fired $ReVO_4$ (Re = La, Ce) microwave dielectric ceramics. J. Am. Ceram. Soc. 2015; 98: 1-4.

[16] Yin CZ, Li CC, Yang GJ, Fang L, Yuan YH, Shu LL, et al. $NaCa_4V_5O_{17}$: A low-firing microwave dielectric ceramic with low permittivity and chemical compatibility with silver

for LTCC applications. J. Eur. Ceram. Soc. 2020; 40: 386-390.

[17] Zhou D, Pang LX, Wang DW, Reaney M, BiVO4 based high k microwave dielectric materials: a review. J. Mater. Chem. C. 2018; 6: 9290-9313.

[18] Zhou D, Guo D, Li WB, Pang LX, Yao X, Wang DW, et.al. Novel temperature stable high-ε_r microwave dielectrics in the Bi_2O_3-TiO_2-V_2O_5 system. J. Mater. Chem. C. 2016; 4: 5357-5362.

[19] Umemura R, Ogawa H, Ohsato H, Kan A, Yokoi A, Microwave dielectric properties of low-temperature sintered $Mg_3(VO_4)_2$ ceramic. J. Eur. Ceram. Soc. 2005; 25: 2865-2870.

[20] Umemura R, Ogawa H, Yokoi A, Ohsato H, Kan A, Low-temperature sintering-microwave dielectric property relations in $Ba_3(VO_4)_2$ ceramic. J. Alloys Compd. 2006; 424: 388-393.

[21] Cheng K, Li CC, Yin CZ, Tang Y, Sun YH, Fang L, Effects of Sr^{2+} substitution on the crystal structure, raman spectra, bond valence and microwave dielectric properties of $Ba_{3-x}Sr_x(VO_4)_2$ solid solutions. J. Eur. Ceram. Soc. 2019; 39: 3738-3743.

[22] Song XQ, Du K, Li J, Lan XK, Lu WZ, Wang XH, et al. Low-fired fluoride microwave dielectric ceramics with low dielectric loss. Ceram. Int. 45 2019 279-286.

[23] Guo HH, Zhou D, Pang LX, Qi ZM, Microwave dielectric properties of low firing temperature stable scheelite structured (Ca, Bi) (Mo, V)O_4 solid solution ceramics for LTCC applications. J. Eur. Ceram. Soc. 2019; 39: 2365-2373.

[24] Li WB, Zhou D, Xi HH, Pang LX, Yao X, Alford N, Structure, infrared reflectivity and microwave dielectric properties of $(Na_{0.5}La_{0.5})MoO_4$-$(Na_{0.5}Bi_{0.5})MoO_4$ ceramics. J. Am. Ceram. Soc. 2016; 99: 2083-2088.

[25] Pang LX, Zhou D, Wang DW, Zhao JX, Liu WG, Yue ZX, et al. Temperature stable $K_{0.5}(Nd_{1-x}Bi_x)_{0.5}MoO_4$ microwave dielectrics ceramics with ultra-low sintering temperature. J. Am. Ceram. Soc. 2018; 101: 1806-1810.

[26] Jesse J, Brown JR, Phase equilibria in the system SrO-CdO-V_2O_5. J. Am. Ceram. Soc. 1972; 55: 500-503.

[27] Joung MR, Kim JS, Song ME, Nahm S, Paik JH, Formation process and microwave dielectric properties of the $R_2V_2O_7$ (R = Ba, Sr, and Ca) ceramics. J. Am. Ceram. Soc. 2009; 92: 3092-3094.

[28] Fukuda K, Kitoh R, Awai I, Microwave characteristics of TiO_2-Bi_2O_3 dielectric resonator, Jpn. J. Appl. Phys. 1993; 32: 4584-4588.

Table 1 Comparison of calculated and theoretical values, sintering temperature, and microwave dielectric properties of $Sr_{3-y}V_2O_{8-y}$ ceramics

y	The volume fraction of $Sr_2V_2O_7$		Theoretical density (g/cm^3)	Relative density (%)	Optimum sintering temperature (^oC)	Dielectric properties		
	Calculation from Fullprof (%)	Theoretical Values (%)				ε_r	$Q\times f$ (GHz)	τ_f (ppm/^{o}C)
0.2	20.47	17.88	4.39	96.36	1000	11.8	36,400	48.7
0.4	37.19	36.70	4.31	97.21	1000	10.6	34,960	20.6
0.6	57.48	56.51	4.24	98.11	950	9.8	27,550	-1.1
0.8	81.31	77.67	4.14	98.55	950	9.4	24,100	-20.1

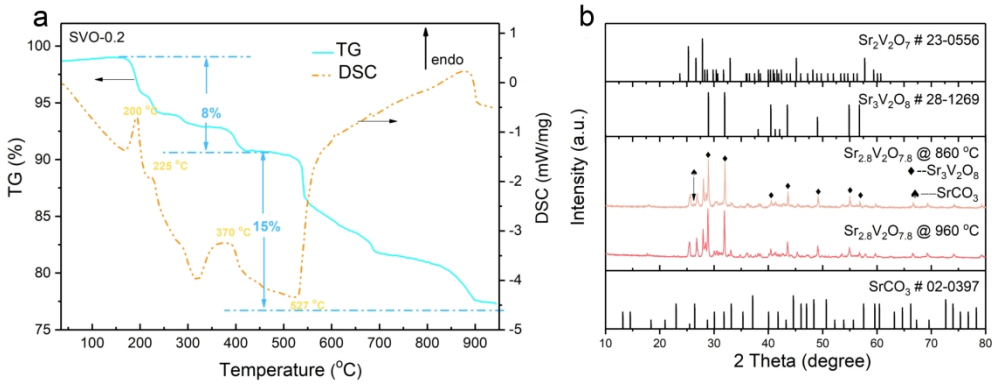

Figure 1 (a) TG/DSC analysis of the y = 0.2 sample, (b) XRD patterns of Sr3-yV2O8-y (y = 0.2) sintered at 860 oC and 960 oC.

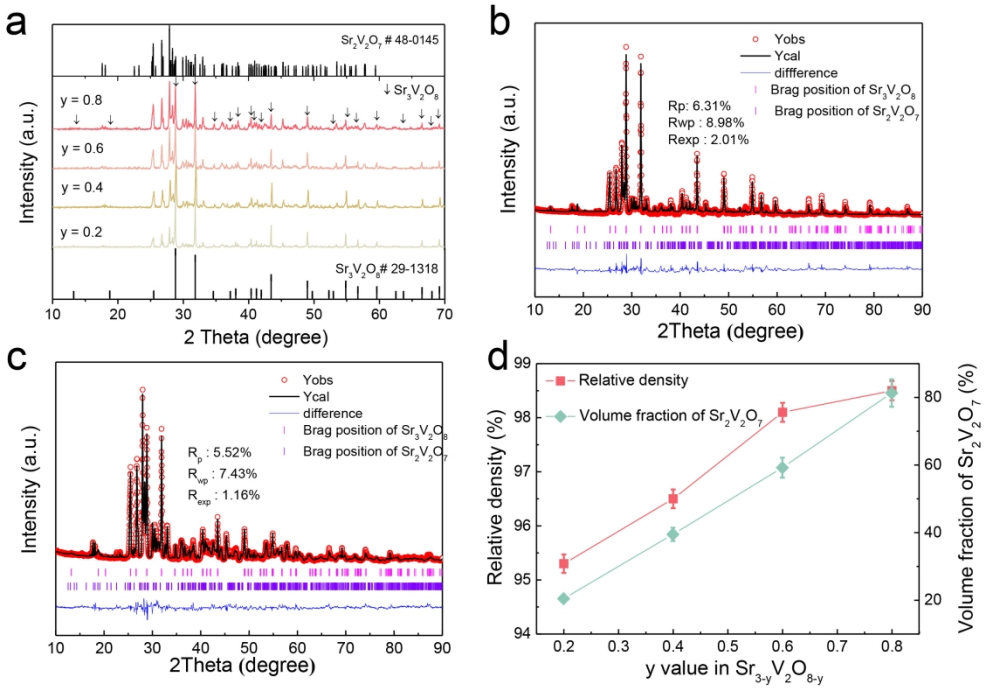

Figure 2 (a) XRD patterns of the Sr3-yV2O8-y (y = 0.2, 0.4, 0.6, and 0.8) sintered at optimum temperature, (b) Rietveld refinement profiles for y = 0.2, and (c) for y = 0.8 and (d) change of phase fraction of Sr2V2O7 calculated from refinement.

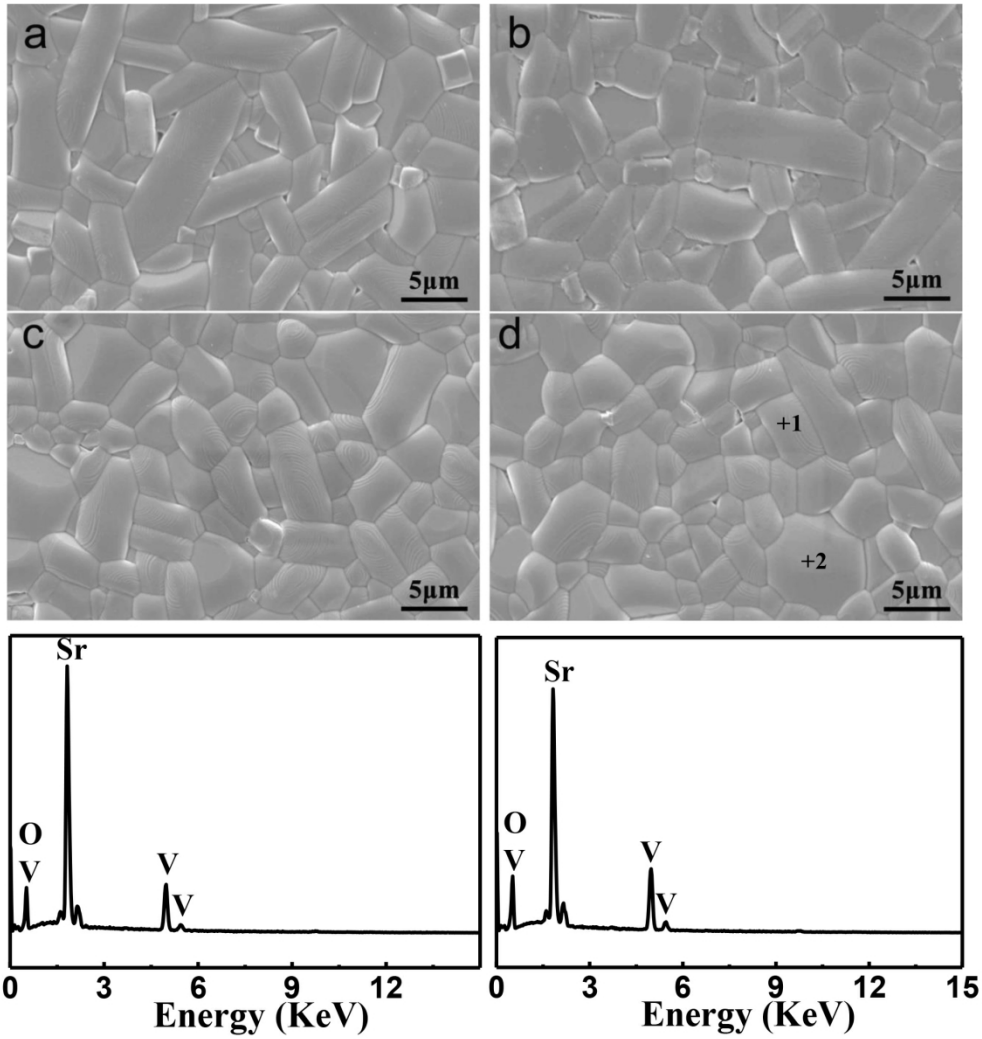

Figure 3 SEM images recorded on the polished and thermally etched surfaces of Sr3-yV2O8-y ceramics: (a) y = 0.2, (b) y = 0.4, (c) y = 0.6, (d) y = 0.8; (e) and (f) EDS for spot 1 and 2, respectively.

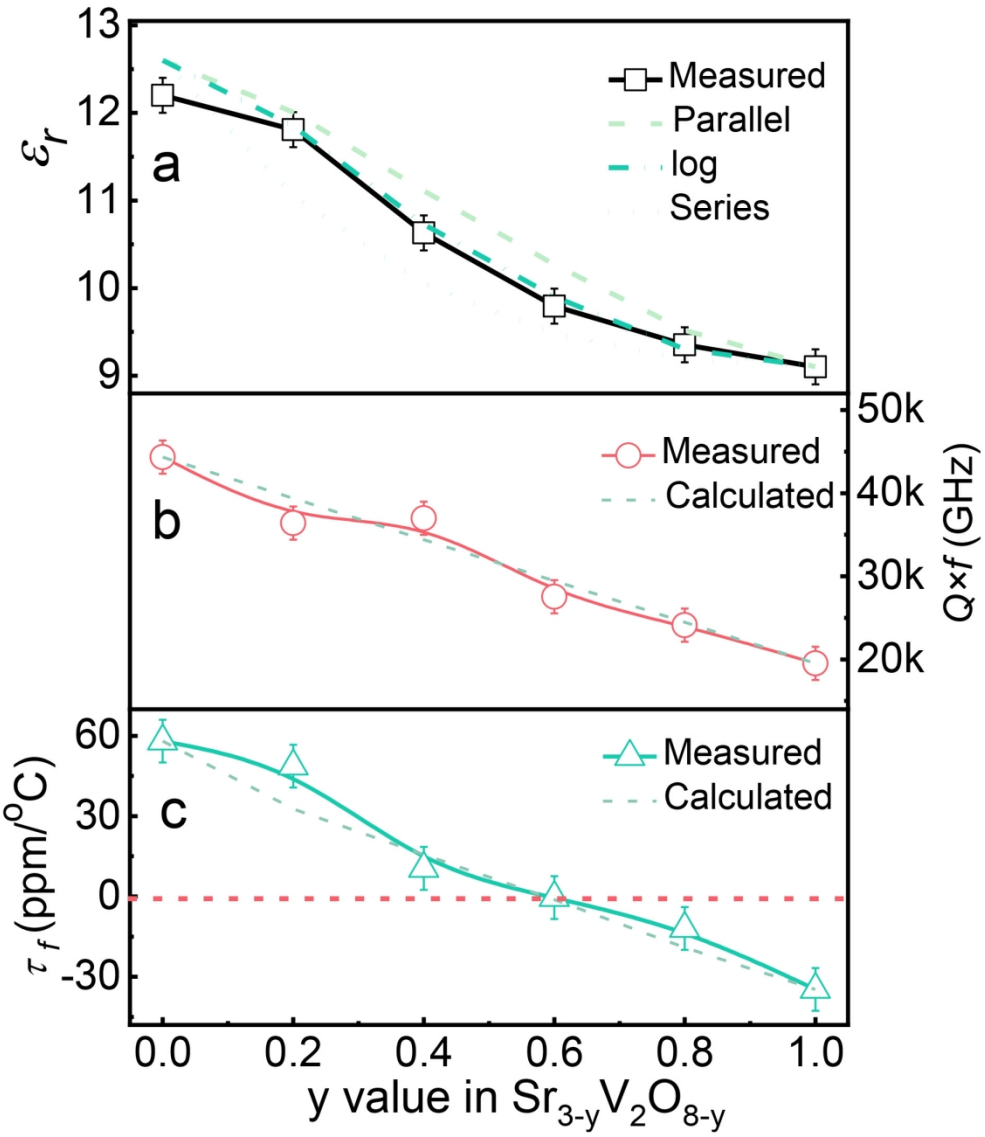

Fig. 4 Variations in microwave dielectric properties as a function of y in the Sr3-yV2O8-y ceramics; the corresponding calculated values are also given for comparison.

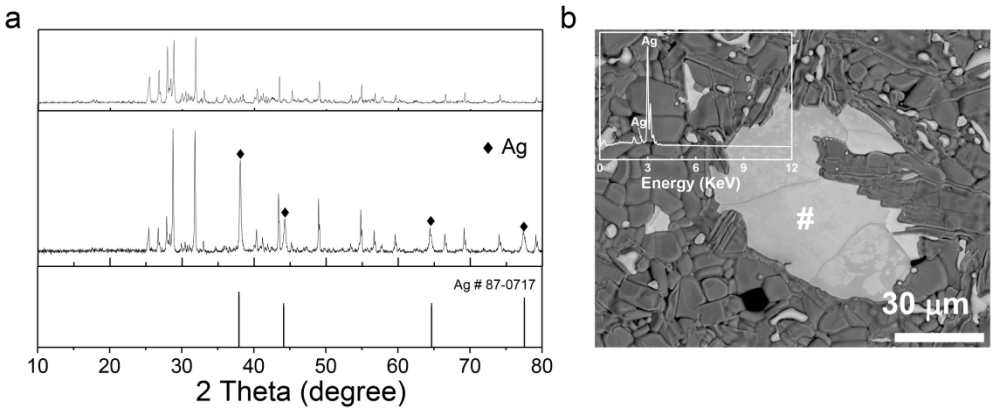

Figure 5 (a) XRD patterns and (b) SEM micrograph of Sr2.4V2O7.4 + 20 wt.% Ag powders at 950 °C for 2 h (EDS analysis of Ag is shown in the inset of Fig. 5(b)).